Janus adhesive dressing with macro/micro dual design enabling sequential microenvironment regulation for scarless wound healing

Meimei Fu,^{1,#} Yue Li,^{1,#} Yitao Zhao,^{4,#}, Yuting Zhu,¹ Zhou Fang,¹ Zhuoyi Huang,^{1,2} Wenjun Luo,¹ Xinyu Huang,¹ Jintao Li,⁴ Zhiqi Hu,^{1,*} Keke Wu,^{3,*} and Jinshan Guo^{1,2,*}

Meimei Fu, Yue Li and Yitao Zhao have contributed equally to this work.

^{*}Corresponding authors: Jinshan Guo: <u>jsguo4127@smu.edu.cn</u>; Keke Wu: <u>drwukeke@126.com</u>; Zhiqi Hu: <u>huzhiqidr163@i.smu.edu.cn</u>.

¹ Department of Histology and Embryology, School of Basic Medical Sciences, Department of Plastic and Aesthetic Surgery, Nanfang Hospital of Southern Medical University, Southern Medical University, Guangzhou, 510515, P. R. China.

² CAS Key Laboratory of High-Performance Synthetic Rubber and its Composite Materials, Changchun Institute of Applied Chemistry, Chinese Academy of Sciences, 5625 Renmin Street, Changchun, 130022, P. R. China.

³ School of Biomedical Engineering, Affiliated Cancer Hospital & Institute, Guangzhou Medical University, Guangzhou, 511495, P. R. China.

⁴ Department of Sports Medicine, Center for Orthopedic Surgery, Orthopedic Hospital of Guangdong Province, The Third School of Clinical Medicine, Southern Medical University, The Third Affiliated Hospital of Southern Medical University, Guangzhou, 510630, P. R. China.

1 Experimental section

1.1 Materials

Silk was purchased from Guangzhou Zhuosheng Biotechnology Co., Ltd. (Guangzhou, China). (-)-Epigallocatechin gallate (EGCG) was purchased from Meryer Chemical Technology Co., Ltd. (Shanghai, China). Formic acid, CaCl₂ and ZnCl₂ were all from Macklin Reagent. All chemicals were analytical reagents and used as received.

1.2 Preparation of Degummed Silk Fibroin

Degummed silk fibroin was prepared according to previous literatures[1]. Briefly, 10 g NaHCO₃ was dissolved in 2 L distilled water and charged to a beaker and heated to ~ 100 ° C. 10 g chopped silkworm cocoons were added and boiled for 30 mins while stirring continuously. Then the silk was washed with distilled water 4-5 times to remove sericin and residual NaHCO₃ to obtain degummed silk fibroin after drying.

1.3 Preparation of Calcium-modified Silk Fibroin (SC) and Calcium/zinc-modified Silk Fibroin Adhesive (SCZ)

Pre-determined amounts of silk fibroin (SF), CaCl₂, and ZnCl₂ with the weight ratios listing in **Table S1** were dissolved in formic acid. For example, to obtain a SCZ_{25/5} adhesive film with a weight ratio of SF: Ca²⁺: Zn²⁺ = 70: 25: 5, for 1 g SF in 10 mL formic acid, 0.991 g CaCl₂ (containing 0.357 g Ca²⁺) and 0.149 g ZnCl₂ (containing 0.071 g Zn²⁺) were dissolved in and used for electrospinning or directly drying in a teflon disk to form an adhesive film. During electrospinning, a 10 mL syringe containing SCZ solution was attached to a needle with a diameter of 0.5 mm, and electrospinning was performed at a constant flow rate of 0.5 mL/h under 15 kV, the distance between the collector and the needle tip was maintained at 15 cm. Then a uniform and transparent SCZ adhesive film was collected and the solvent was completely evporated.

1.4 Preparation of All-in-one Silk Fibroin-based Janus Adhesive Dressing (SCE)

SCE was prepared via coaxial electrospinning at room temperature, with SF solution with different concentrations of EGCG as the core solution and pure SF solution as the shell solution. During electrospinning, a 10 mL syringe containing the SF-EGCG solution was connected to an inner needle with a diameter of 0.33 mm, and a 30 mL syringe filled with SF solution was connected to an outer needle with a diameter of 1.07 mm. The two solutions were separately connected into different micro-pumps for coaxial electrospinning to prepare core-shell electrospun Janus adhesive dressing on top of SCZ. The optimized condition with distance between the collector and the needle tip being maintained at 15 cm and the electric voltage and flow rate being kept as 15-20 kV and 0.1-0.5 mL/h, respectively, was used in the electropinning process. The nomenclature and composition of different core-shell electrospinning fibers are shown in **Table** S2. The preparation of SCE involves a multi-step process: firstly, SCZ are prepared through Ca²⁺/Zn²⁺ modified SF, followed by SE spinning on the upper surface of SCZ using coaxial electrospinning technology, ultimately forming SCE double-layer dressing. In the subsequent experiments, the main experimental groups included: 1) unmodified silk fibroin group, 2) dual-ion adhesive layer (SCZ), 3) core-shell structured fiber layer (SE_x, x means x% of EGCG), and 4) bilayer Janus adhesive dressings incorporating different concentrations of epigallocatechin gallate (EGCG) (designated as SCE₁, SCE₅, and SCE₁₀).

1.5 Characterizations of Adhesive Dressings

The core-shell structure of the upper layer electrospinning fiber was observed using TEM (FEI TecnaiG2 20 S-Twin) and laser scanning confocal microscope (LSCM, Carl Zeiss, Germany, with rhodamine B in the core layer and calcein in the shell layer). In addition, the morphology and microstructure of all SCEs were observed by scanning electron microscopy (SEM, Quanta 200,

Japan), and the dispersion of different elements in SCE was also examined using energy dispersive spectroscopy (EDS) elemental mapping. FTIR (Thermo Scientific, Nicolet-iS10) was used to study the chemical compositions of the prepared adhesive dressings. Meanwhile, the thermal stability of the silk fibroin dressing films was studied by differential scanning calorimetry (DSC) under nitrogen atmosphere.

1.6 Contact Angle and Water Vapor Transmission Rate Measurement of SCE

Contact angle test: The dynamic contact angle of the SCE dressing was measured by an optical contact angle measuring instrument (JY-82B Kruss DSA, China), using a testing droplet of 5 µL [2]. The timer starts when the droplet first touched the surface of the sample and separated from the needle tip. Images were captured and the contact angle was recorded using a Charge Coupled Device (CCD) camera. At least three specimens were tested for each sample and the results were averaged.

Water vapor transmission rate measurement: The water vapor transmission rate (WVTR) was measured using a moisture permeability cup. Briefly, a sufficient amount of water was added in the moisture permeability cup at room temperature, and the cup was covered precisely with a circular dressing film. Then the sample was sealed with a clamp plate and fasten with clips to form a watertight seal between the clamp plate and the lid. The container and sample were weighed and recorded (W₁). The container was placed in a drying oven or incubator with the sample facing up and maintained a temperature of $37 \pm 1^{\circ}$ C. After 18 to 24 hours, each container was removed from the drying oven or incubator, recorded the test time (T), and immediately re-weighed the container, sample, and liquid, recorded the mass (W₂) to an accuracy of 0.0001g. The WVTR was finally calculated using the following formula (1):

WVTR =
$$((W_1 - W_2)*1000 \times 24)/T$$
 (1)

In the formula: the unit of WVTR is in grams per square meter per 24 hours (g/m^2 24h); W_1 is the initial mass of the container, sample, and liquid in grams (g), W_2 is the mass of the container, sample, and liquid after the test period in grams; T is the test duration in hours.

1.7 Adhesion Strengths of SCZ and Peeling Strengths of SCE

Adhesion strength: First, the universal adhesion of SCZ to various substrates, including metal, glass, rubber, and plastic, was demonstrated. Besides, the adhesion strength of SCZ against wet tissue was measured according to the modified American Society for Testing and Materials (ASTM) F2255-05 method.[3] Briefly, porcine skin was soaked in 1 mol/L sodium hydroxide solution to remove the inner fat layer, washed with deionized water, and then cut into rectangular strips (length × width = 30 mm × 10 mm). An appropriate amount of SCZ film was applied to the ends of two porcine skin substrates adhered on glass slides, overlapped to form an overlap area of 10×10 mm² lap shear joint, and cured for 2 hours at 37°C and 50% humidity. Lastly, the adhered tissue was stretched using a universal testing machine (Instron 34TM-10) equipped with a 10 N load cell at a constant stretching rate of 5 mm/min, until failure. The adhesion strength was calculated by dividing the maximum load (force) with the overlap contact area. For each sample, at least 8 specimens were tested, and the results were averaged.

Peeling strength: The peel strength of SCE dressing was measured through a 180° peel test using a mechanical testing machine (Instron 34TM-10). Simply, the SE dressing was cut into rectangle shaped specimens (length × width = 30 mm × 10 mm). Then, added SC or SCZ on the edge of SE and overlapped to form an overlap area of 10 × 10 mm ²adhesion area, and cured for 2 hours at 37°C and 50% humidity. Finally, the edge of the SE dressing was fixed in the upper z-axis stage and detached at 180° angle with a peeling speed of 5 mm/min. The peel strength was estimated by dividing the measured peeling force with the SCZ dressing adhered width.

1.8 Mechanical Property of SCE

The mechanical property of SCE dressing was measured using an Instron 34TM-10 testing machine with a 500 N load cell according to ASTM standard D412A. The SCE dressing was cut into rectangle shaped specimens (length \times width = 30 mm \times 10 mm), which were elongated to failure at 50 mm/min. The Young's modulus was calculated by measuring the gradient from 0 to 10% of the stress-strain curve. For each sample, eight specimens were tested and the results were averaged.

1.9 In Vitro Degradation and Release Experiments

Degradation experiment: The dressing was immersed in 0.1 M PBS solution at 37 ℃, and the degradation status of SF, SCZ, SE₅ and SCE dressings was photographed at the predetermined time point (0, 0.1 h, 0.5 d, 1 d, 1.5 d, 2 d, 3 d, 4 d, 5 d, 6 d, 7 d, 8 d).

In vitro EGCG release: The tresswell chamber was used to simulate the practical use of the adhesive dressing on the wound, in which the adhesive film in the lower layer of SCE degraded first, then the upper layer of SCE degraded and released EGCG. Briefly, the SCE was cut to a suitable size and was closely attached to the transwell chamber. Then, the transwell chamber was soaked in 200 μ L PBS solution in a 24-well plate at 37 $\,^{\circ}$ C (the solution just closed over the lower layer of SCE). The concentration of released EGCG was measured at pre-determined time points (0, 0.25, 0.5, 1, 2, 3, 5, 7, 10, 14, 18 days) using a UV-visible spectrophotometer (Shimadzu, UV-2600). And the concentrations of released Ca²⁺and Zn²⁺ were also measured by ICP-MS (iCAP PRO, Thermo Fisher Scientific, MA, USA).

1.10 In Vitro Biocompatibility Experiments

Cytotoxicity, cell proliferation, 2D (scratch) and 3D (transwell) cell migration assay experiments were conducted on the adhesive dressings to assess the cytocompatibility of the

dressings. In accordance with the national GBT 16886.1-2022 medical device biological evaluation standards, different extraction solutions of SF, SCZ, SE and SCE adhesives were prepared by extracting various dressing films using a complete culture medium (DMEM medium containing 10% fetal bovine serum and 1% penicillin-streptomycin) at 6 cm 2 /mL. The obtained 1× extraction solution was then diluted 10 or 100 times by complete culture medium to give 10× and 100× extraction solutions, respectively. The cytotoxicity of EGCG-containing complete culture media with gradient concentrations and the extraction solution of different adhesives against mouse fibroblasts (L929) and human umbilical vein endothelial cells (HUVEC) was studied using the CCK-8 assay. Briefly, L929 and HUVEC cells were cultured in DMEM medium containing 10% fetal bovine serum and 1% penicillin-streptomycin at 37 °C and 5% CO₂, followed by being seeded in a 96-well plate at a density of approximately 4×10^4 cells/well. After 24 hours, the original culture medium was discarded, replaced with EGCG-containing medium or various extraction solutions with different dilutions, and incubated for another 24 hours before the CCK-8 assay test by measuring the OD value at 450 nm using a microplate reader. The cell viability was calculated using the following formula (2):

Cell viability (%) =
$$(Ab_{sample} - Ab_{blank}) / (Ab_{control} - Ab_{blank}) \times 100$$
 (2)

Where Ab_{sample} was the absorbance of the sample at 450 nm, Ab_{control} is the absorbance of the control at 450 nm, and Ab_{blank} is the absorbance of the blank well without cell at 450 nm.

To evaluate the effect of adhesive dressing on the adhesion and proliferation of L929 cells, both CCK-8 assay and Live/Dead staining were conducted. Following the same steps as the cytotoxicity tests, L929 cells are seeded in 96 and 24-well plates and cultured for 1, 3, and 5 days, with the medium containing different extraction solutions (1×) being changed every other day. At predetermined time points, the OD values of the solutions in the 96-well plates are measured.

Additionally, cells in the 24-well plates are stained according to the Live/Dead staining kit instruction and cell morphology was observed and photographed using an inverted fluorescence microscope (Olympus CKX41, Tokyo, Japan).

The effect of the adhesive dressings to the cell migration capability was evaluated by both 2D (scratch) assay and 3D (transwell) cell migration assay, using the $1\times$ extraction solution of different samples. The L929 cells at $(1\times10^5 \text{ cells/mL})$ were seeded in a 24-well plate with an amount of 100 µL per well. After incubation for 24 hours in complete culture medium to allow cell adhesion and monolayer formation, vertical scratches were made at the bottom of the well by a 1 mL pipette tip. Then, the suspended cells were washed with sterile PBS (pH 7.4) three times, and the remaining cells were cultured in complete culture medium for 24 and 48 hours. Meanwhile, photos of cell scratches were taken using an inverted optical microscope (Olympus CKX41, Tokyo, Japan). Tests of each group were repeated three times. The cell migration rate was quantitatively calculated by and the following formula (3):

Migration rate (%) =
$$(W_i - W_t)/W_i \times 100$$
 (3)

Here, W_i denotes the initial scratch width at 0 h, W_t represents the scratch width after being cultured for t hours (t = 24 or 48).

For transwell assay, the transwell chambers (Corning, 353097) were put into the wells of 24-well plates containing complete DMEM culture medium (control) or 1×extraction solution. L929 cells with a density of 5×10⁴ cells/mL were seeded in the chambers (200 μL/chamber) and cultured for 24 hours. Then the cells on the upper surface of the chamber were completely removed by wiping with a cotton swab, and the cells on the lower surface were subsequently fixed with 4% paraformaldehyde solution for 15 minutes and stained with crystal violet for another 15 minutes, followed by washing with sterile PBS, and being observed and photographed with an inverted

optical microscope (Olympus CKX41, Tokyo, Japan). Then the chamber was immersed in 33% glacial acetic acid for elution, and the OD value of the eluted solution at 570 nm was measured.

1.11 In Vitro Antioxidant and Anti-inflammatory Effect of SCE

The antioxidant and anti-inflammatory effect of SCE was investigated by conducting 2,2-diphenyl-1-picrylhydrazyl (DPPH) scavenging experiment, the intracellular reactive oxygen species (ROS) assay against mouse fibroblasts (L929 cells) and the expression experiments of inflammatory factors (IL-1 β and IL-6) by human dermal fibroblasts (HDFs).

DPPH scavenging experiment: Different dressing films with fixed area of 3 mm² were added to the DPPH solution in methanol (4 mL, 100 μM). After incubating under the dark for 30 min, the absorbance (A_s) of the solution at 517 nm was measured using a UV-Vis spectrophotometer (Shimadzu, UV-2600). In addition, a representative dressing, SCE₅, was used to determine the absorbance after incubation for different times. The absorbance of the untreated DPPH solution (A_c) was used as a blank control. The DPPH scavenging rate was calculated using the following formula (4):

DPPH scavenging (%) =
$$(A_c - A_s)/A_c \times 100$$
 (4)

Intracellular ROS scavenging experiment: Briefly, L929 cells were seeded into 24-well plates and incubated at 37 ° C for 24 hours. All groups except the blank group (untreated) underwent 2-hour hydrogen peroxide (H₂O₂) stimulation to establish the inflammation model. Then, the original medium was discarded and the complete medium containing the 1×extraction solution of dressing was added and the cells were incubated for another 6 hours. After discarding the medium and washing with sterile PBS twice, a 2',7'-dichlorodihydrofluorescein diacetate (DCFH-DA) solution was added, and the cells were incubated for 20 minutes. Cells were observed and photographed with an inverted fluorescence microscope (Olympus CKX41, Tokyo, Japan) after

washing with sterile PBS. L929 cells treated solely with H₂O₂ were set as the positive control group, and untreated cells were served as the blank group [4].

Expression of the inflammatory factor: The IL-1β and IL-6 cytokines expression in human dermal fibroblasts (HDFs) treated with the 1x extraction solution of dressings were assessed using cellular immunofluorescence staining. HDFs were cultured in complete DMEM under 37 °C, 5% CO₂ until optimal fusion was achieved. Subsequently, cells were cultured in complete DMEM containing the extraction solution of dressing (1/10 to complete DMEM c(v/v)) for 24 hours. Except for the blank group, all other groups were pretreated with lipopolysaccharide (LPS). After 24 hours, the cells were fixed with 4% paraformaldehyde for 15 mins and incubated in QuickblockTM immune blocking solution for 1 hour. Following this, the rabbit anti-IL-1β or rabbit anti-IL-6 antibodies (diluted to a ratio of 1:50) from HUABIO (China) were added and further incubated overnight at 4 °C. Then, DyLing488 Conjugate goat Anti-rabbit IgG (diluted to a ratio of 1:200, Abbkine, China) was added and incubated in darkness for 1 hour. Finally, the cellular nuclei were labeled with 4', 6-diamidino-2-phenylindole (DAPI) reagent. The fluorescence images were observed and photographed by an inverted fluorescence microscope (Olympus CKX41, Tokyo, Japan) and semi-quantitative analysis was performed using Image J.

1.12 In Vitro Antiangiogenesis of SCE

The effect of SCE on angiogenesis was systematically evaluated by tube formation assay and expression of vascular-related factors (CD31 [platelet endothelial cell adhesion molecule-1]c, VEGF [vascular endothelial growth factor]) using human umbilical vein endothelial cells (HUVEC).

Tube formation assay: Berifly, 100 μL of Matrigel (Corning, 356234) was added and gently shaken to cover the bottom of each well in 48-well plates. The culture plate was then incubated for

more than 1 hour at 37 $^{\circ}$ C to solidify the matrix glue. HUVEC cells were seeded on the matrix gel at a density of 2 \times 10⁴ cells/mL, along with 1/10 volume of the extract solution, and then cultured at 37 $^{\circ}$ C with 5% CO₂ for 6 hours. The formation of celltubes was observed and photographed with an inverted microscope, and the average relative length of the cell tubes was quantitatively analyzed using ImageJ software.

Expression of the the vascular-related y factor: The effect of the expression levels of CD31 and VEGF in HUVEC cells after being treated with the extract of dressings was assessed using cellular immunofluorescence staining. HUVEC cells were cultured in DMEM at 37 °C, 5% CO2 until optimal fusion was achieved. Subsequently, HUVECs were cultured in complete DMEM containing the extraction solution of dressing (1/10 to complete DMEM (v/v)) for 24 hours. Then the cells were fixed with 4% paraformaldehyde for 15 min and incubated in QuickblockTM immune blocking solution for 1 hour. Following this, the rabbit anti-CD31 or rabbit anti-VEGF antibodies (diluted to a ratio of 1:50) from HUABIO (China) were added and further incubated overnight at 4 °C. Then, DyLing488 Conjugate goat Anti-rabbit IgG (diluted to a ratio of 1:200, Abbkine, China) was added and incubated under darkness for 1 hour. Finally, the cellular nuclei were labeled with DAPI. The fluorescence images were observed by an inverted fluorescence microscope (Olympus CKX41, Tokyo, Japan) and semi-quantitative analysis was performed using Image J.

1.13 The Antibacterial activity of SCE

The antibacterial activity of the dressing was evaluated using *Escherichia coli* (ATCC 8739) and *Staphylococcus aureus* (ATCC 6538) as representative Gram-negative and Gram-positive bacterial strains, respectively. Briefly, sterilized circular dressing samples (10 mm in diameter) were placed in sterile EP tubes, inoculated with 2 mL bacterial suspension (1×10⁶ colony forming

units (CFUs)/mL), and co-cultured at 37 $^{\circ}$ C for 24 hours, with untreated bacterial suspension serving as negative control. After incubation, optical density (OD) at 600 nm was measured using a microplate reader. Additionally, 20 μ L of 100-fold diluted bacterial suspension was evenly spread on agar plates and cultured at 37 $^{\circ}$ C for 24 hours to further observe the antibacterial efficacy. All experiments were performed in triplicate, with data being presented as mean \pm standard deviation.

1.14 In Vivo Hemostatic Capacity of SCE

Male Sprague-Dawley rats (200 g) were used to evaluate hemostatic efficacy in both the liver incision model and the tail amputation model. The animals were randomly divided into three groups (n=3 per group): Control, SCZ-treated, and SCE₅-treated groups. Following intraperitoneal anesthesia with sodium pentobarbital (2% w/v, 50 mg/kg), rats were secured on a surgical platform. For the liver incision model, a midline laparotomy was performed to expose the liver, and after clearing surface exudate, a standardized wound (3 mm depth × 7 mm length) was created on the left lobe using a microsurgical scalpel, followed by immediate application of the dressing membrane. In the tail amputation model, complete transection at the fifth caudal vertebra was performed with immediate full coverage by the dressing. For both models, pre-weighed filter papers were used to absorb hemorrhagic exudate until active bleeding ceased, after which the dressing was removed and re-weighed to calculate total blood loss by gravimetric difference. All experiments were performed in triplicate, with data being presented as mean ± standard deviation.

1.15 In Vivo Wound Healing Experiments

Creation of full-thickness wound model and general processes of wound healing: A full-thickness wound model was established on the back of Sprague Dawley (SD) rats to evaluate the *in vivo* wound healing effect of SCE. SD rats (200g, male) were purchased from the Experimental

Animal Center of the Experimental Animal Center of Southern Medical University. All animal procedures were approved by the Animal Experiment Ethics Committee of Nanfang Hospital, Southern Medical University (Approval No.: NFYY-2022-0118) and strictly complied with China's Regulations on the Management of Laboratory Animals and the ARRIVE 2.0 guidelines. The SD rats were randomly divided into six groups (n = 5): Control, SF, SCZ, SE₅, SCE₅, and SCE₁₀. All animals were anesthetized with intraperitoneal injection of sodium pentobarbital (2% w/v, 50 mg/kg), then shaved on the back using an electric animal shaver, and finally the surgical site was fully exposed using depilatory cream. Subsequently, six circular full-thickness wounds (diameter ~15 mm) were created on the back of each rat using surgical scissors. After removing the wound skin, the wounds were covered with dressings, with the wounds of the control group being left untreated. Wound photos were taken on day 0, 3, 7, 14, and 21 post-surgery to record the wound healing process and analyzed with Image J.

Histological and Immunohistochemical staining: The treated tissue samples were harvested on day 7, 14, and 21 post-surgery, and fixed overnight in 4% paraformaldehyde, dehydrated in ethanol solutions with graded concentrations, embedded in paraffin, and finally sectioned into 4 μm slices. The tissue slices were assessed by histological (hematoxylin and eosin (H&E), Masson's trichrome, and sirius red) staining, immunohistochemical (interleukin 1-beta (IL-1β), interleukin 10 (IL-10), and transforming growth factor-β (TGF-β)) staining, as well as immunofluorescence (CD31 and α-smooth muscle actin (α-SMA)) staining. The effect of the dressing to the epidermal regeneration, collagen deposition, inflammation, and angiogenesis were observed and semi-quantitatively analysized using an upright fluorescence microscope (Leica DM4000B, Wetzlar, Germany) and Image J, respectively. The *in vivo* safety was assessed by conducting histological

examination of the major organs of the treated rats, including heart, liver, spleen, lung, and kidney, using H&E staining 21 days after surgery.

Rat skin microbiology sample collection, 16s r-RNA sequencing and data analysis: The rat skin microbiology samples were collected from the back of SD rats using sterile cotton swabs and the head of the swabs were immersed in sterile preservation solution and sent to Shanghai Paisano Biological Co. for sequencing. Detailed analysis of 16s-rRNA gene extraction, PCR amplification and sequencing of microbial samples were conducted referring to previously reported literature.

1.16 In Vivo Scar Prevention Experiment on Rabbit Ear

Creation of rabbit ear scar model and general experimental processes: Nine New Zealand white rabbits (3-4 months old) were purchased from the Experimental Animal Center of the Experimental Animal Center of Southern Medical University. All animal procedures were approved by the Animal Experiment Ethics Committee of Nanfang Hospital, Southern Medical University (Approval No.: NFYY-2022-0118) and strictly complied with China's Regulations on the Management of Laboratory Animals and the ARRIVE 2.0 guidelines. New Zealand white rabbits (3-4 months old) were anesthetized with intravenous injection of sodium pentobarbital (3% w/v, 30 mg/kg). Subsequently, three wounds were created on each ear using an 8 mm biopsy punch, and the perichondrium was completely excised with a scalpel. The wounds were treated with sterile PBS (10 µL), SF, or SCE₅ film, respectively. Wound healing progression was photographically documented throughout the treatment period. The experimental animals were randomly allocated into three groups (n = 6 per group), with subsequent collection of treated scar tissues at postoperative days 14, 21, and 28 for histological analyses including hematoxylin and eosin (H&E) staining, Masson's trichrome staining, and picrosirius red staining. All images of tissue sections were documented under a slide scanner microscope (SQS40P, Shengqingkeji, china), and Scar

Elevation Index (SEI) and Epidermal Thickness Index (ETI), the ratio of type I/III collagen and polar coordinates of collagen fiber orientation were analyzed using Image J software.

Transcriptome sequencing and Immunohistochemical staining of rabbit ear wound scar tissue: Postoperative New Zealand rabbit ear wound scar tissues were collected on day 14, 21 and 28 and sent to Shanghai Parsonage Biotech for transcriptome sequencing based on the illumina platform (n = 3 for each group). Based on the R package, the transcriptome data were subsequently visualized and analyzed for GO pathway, KEGG pathway and heat map differential genes. Subsequently, representative cytokines (IL-1α, TNF-α, VEGF, CD31, COL4 and MMP9) were selected for immunohistochemical staining at each stage to verify the transcriptome results.

1.17 Statistical Analysis

All the experimental data were statistically analyzed by GraphPad Prism 9 (GraphPad Software, USA) and expressed as mean \pm standard deviation (SD), and the statistical difference was determined by t-test or one-way ANOVA. For nonparametric data, the Mann Whitey test was used for comparisons between two groups and the Kruskal-Wallis test for comparisons between multiple groups. All the data are considered to have significant differences only when p < 0.05. *, ** and *** represent p < 0.05, p < 0.01 and p < 0.001, respectively.

Table S1. Nomenclature of different lower layer adhesives and the amounts of SF, Ca^{2+} , and Zn^{2+} . 1g SF was dissolved in 10 mL formic acid to form a solution with a concentration of $10 \,_{\text{w/v}}\%$.

Sample	SC ₅₀	SC ₄₀	SC ₃₀	SC_{20}	SC_{10}	SCZ _{20/10}	SCZ _{25/5}	SCZ _{29/1}	SCZ _{29.9/0.1}
SF (g)	1	1	1	1	1	1	1	1	1
$Ca^{2+}/CaCl_{2}\left(g\right)$	1/2.77	0.67/1.85	0.43/1.19	0.25/0.69	0.11/0.31	0.29/0.79	0.36/0.99	0.41/1.15	0.43/1.19
$Zn^{2+}\!/ZnCl_{2}\left(g\right)$	0/0	0/0	0/0	0/0	0/0	0.14/0.3	0.07/0.15	0.014/0.03	0.001/0.002

Table S2. Nomenclature of different upper core-shell electrospinning fibers (SE_x, x means x% of EGCG) and the weight amounts of SF and EGCG used in the core/shell spinning solution. SF was dissolved in formic acid in a concentration of $10 \,_{\text{W/v}}\%$.

Sample	SE _{0.5}	SE_1	SE_5	SE_{10}	SE_{20}	SE ₅₀
SF (core, g)	0.1	0.1	0.1	0.1	0.1	0.1
EGCG (core, mg)	0.5	1	5	10	20	50
SF (shell, g)	0.3	0.3	0.3	0.3	0.3	0.3

Table S3.

Name for a series of all-in-one silk fibroin-based Janus adhesive dressing containing different upper and lower layers.

Sample	SF	SCZ	SE ₅	SCE ₁	SCE ₁	SCE ₁
Number of layers	1	1	1	2	2	2
The upper layer	SF	/	SE_5	SE_1	SE_5	SE_{10}
The lower layer	/	SCZ _{25/5}	/	SCZ _{25/5}	SCZ _{25/5}	SCZ _{25/5}

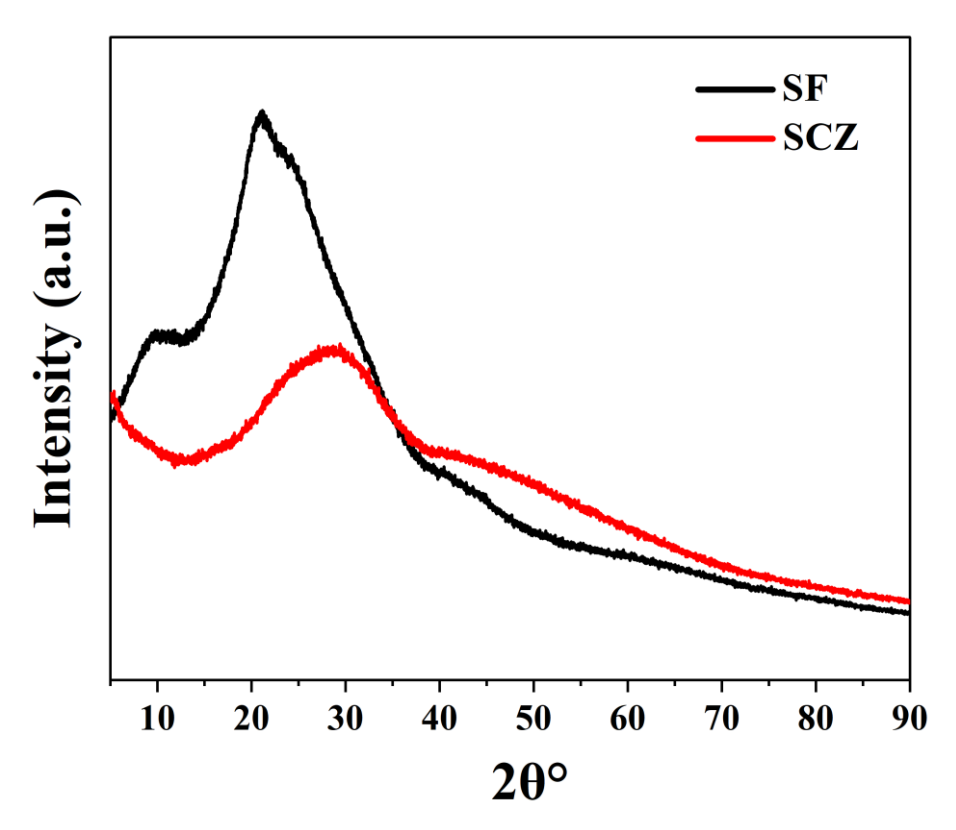


Fig. S1 XRD patterns of SF and SCZ.

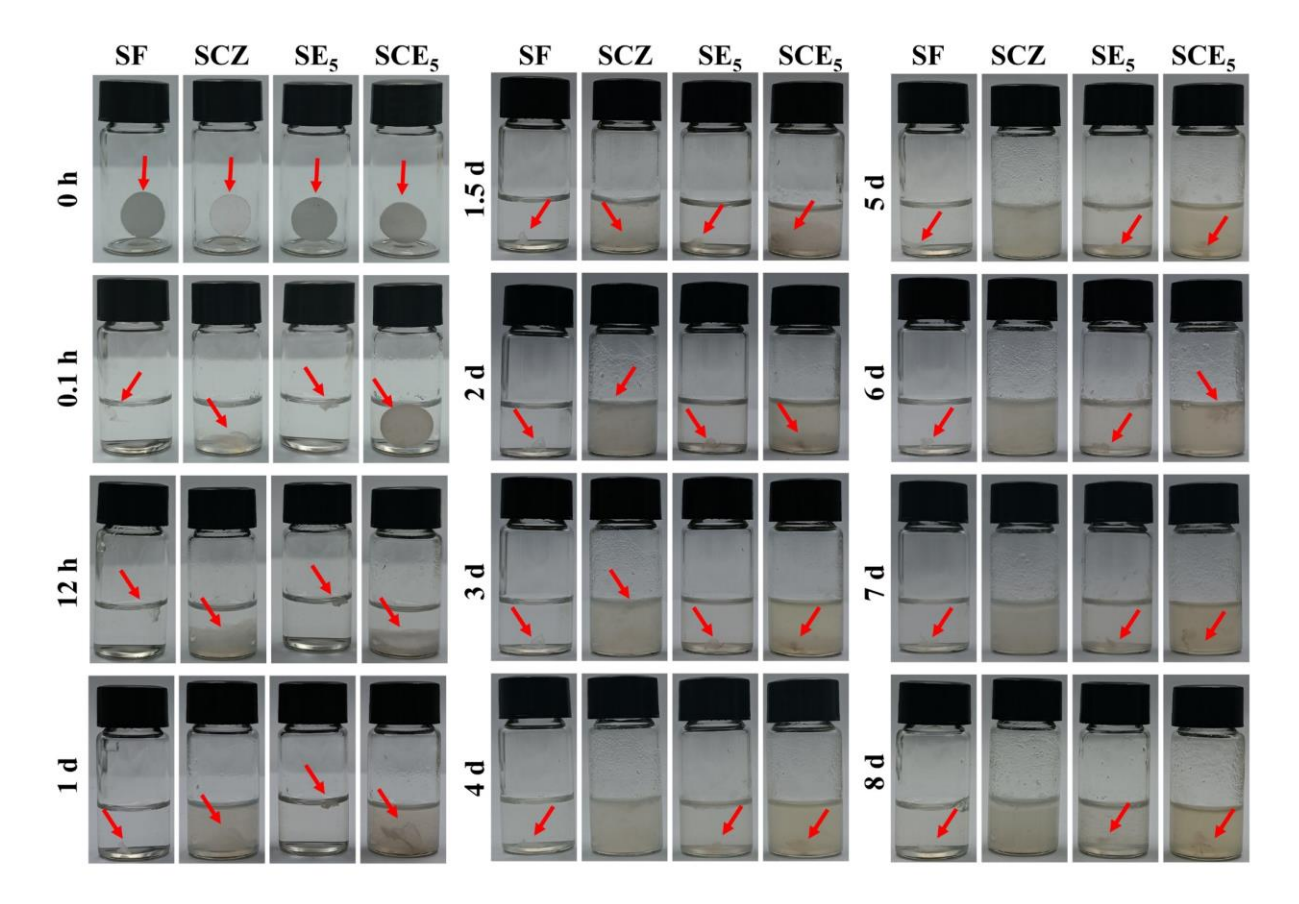


Fig. S2 The degradation photos of SF, SCZ, SE₅ and SCE₅ in PBS at different time points.

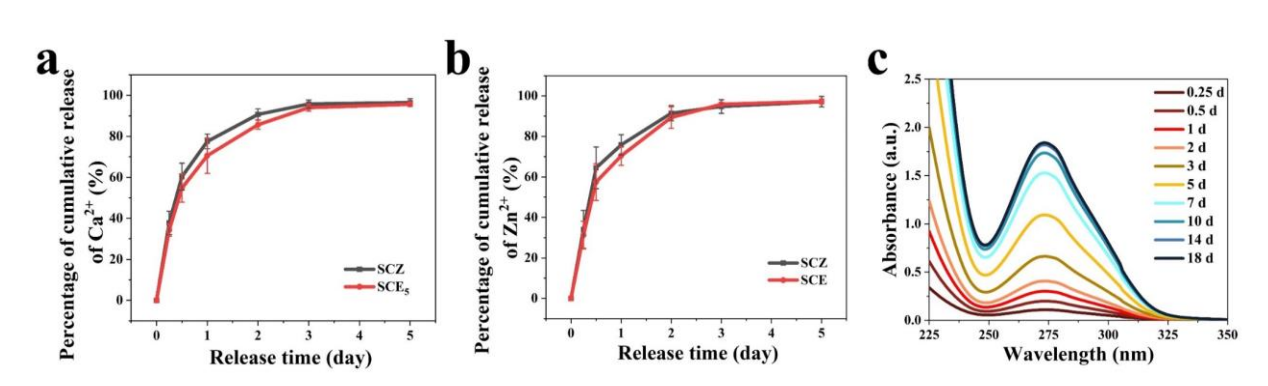


Fig. S3 a Ca²⁺ releasing curves of SCZ and SCE₅. **b** Zn²⁺ releasing curves of SCZ and SCE₅. **c** UV spectra reflecting EGCG release from SCE₅ at different time points.

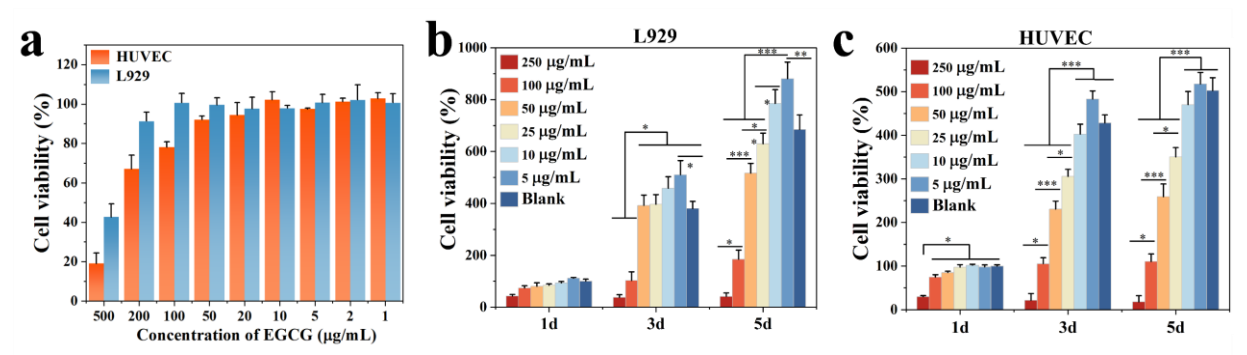


Fig. S4 Cytocompatibility of EGCG: **a** Cell viability of different concentrations of EGCG on L929 and HUVEC cells (n = 4). Cell viabilities of **b** L929 and **c** HUVEC cells on day 1, 3 and 5 (n = 4, using the cell viability of the blank control group on day 1 as 100%). *p < 0.05, **p < 0.01, ***p < 0.001.

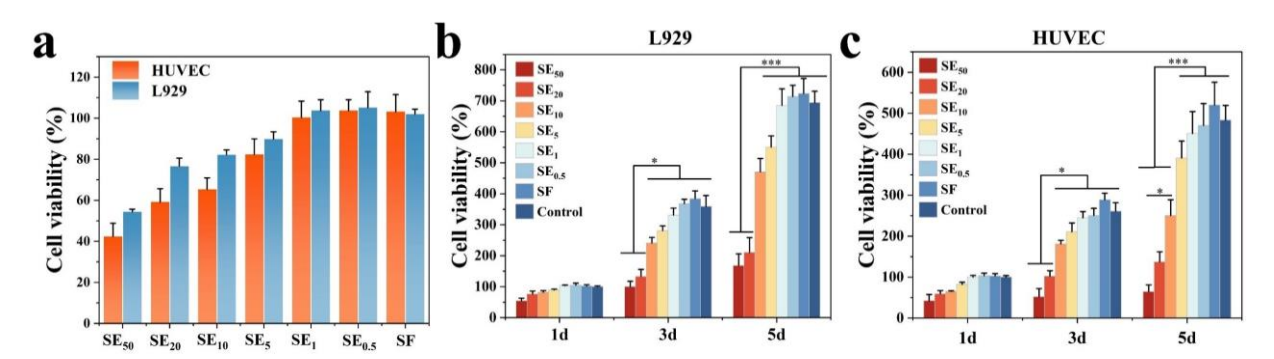


Fig. S5 Cytobiocompatibility of different SE electrospinning films: **a** cell viability of different films against L929 and HUVEC cells (n = 4). Cell viabilities of **b** L929 and **c** HUVEC cells on day 1, 3 and 5 (n = 4, using the cell viability of the blank control group on day 1 as 100%). *p < 0.05, **p < 0.01, ***p < 0.001.

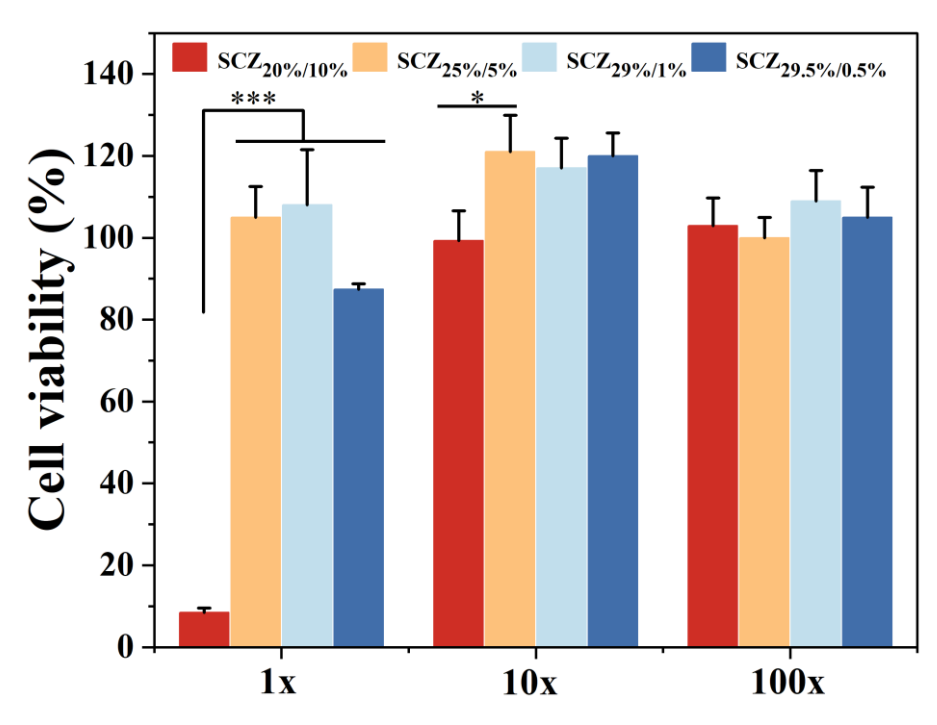


Fig. S6 Evaluation of cytobiocompatibility of SCZ membrane degradation solution with different dilutions (n = 4). *p < 0.05, **p < 0.01, ***p < 0.001.

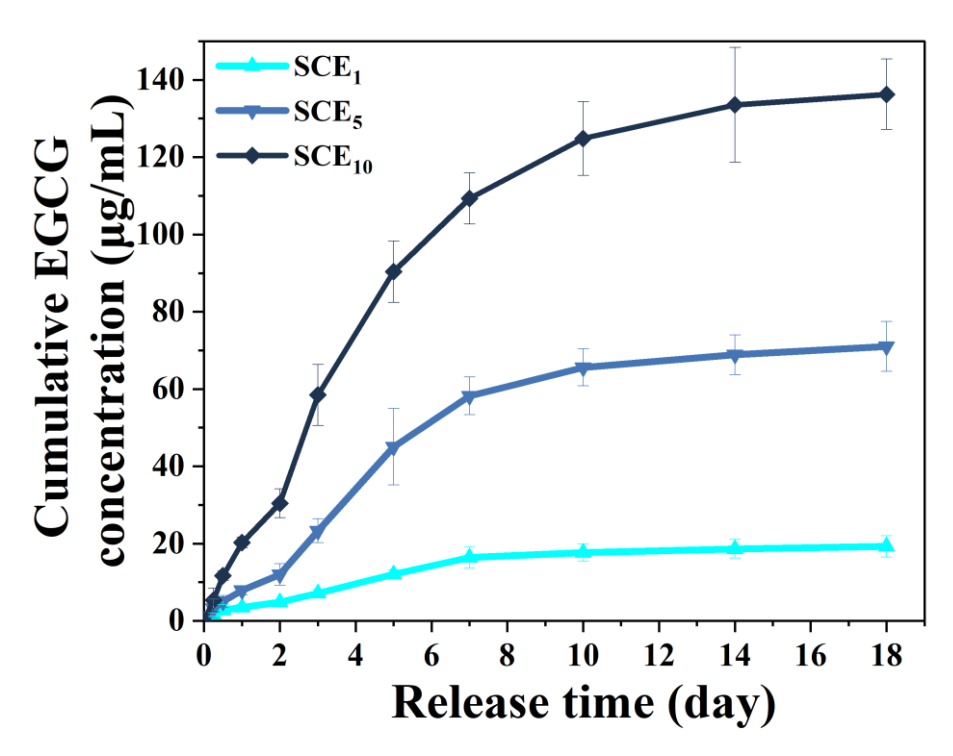


Fig. S7 Cumulative EGCG releasing concentration of SCE_1 , SCE_5 , and SCE_{10} (n = 3).

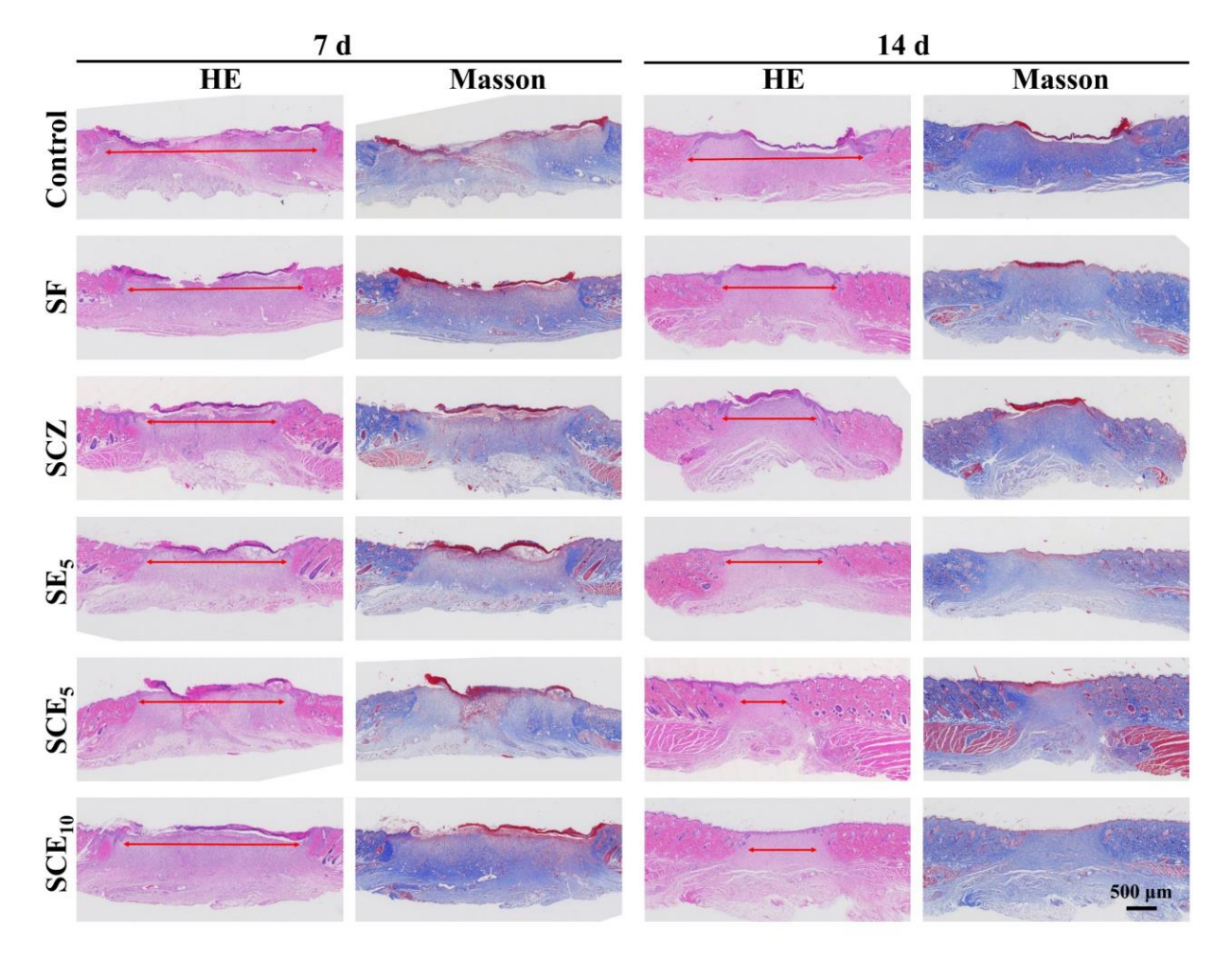


Fig. S8 H&E and Masson staining images of rat skin wound tissues of Control, SF, SCZ, SE₅, SCE₅, SCE₁₀ groups on day 7 and 14 (red arrows indicate wound width).

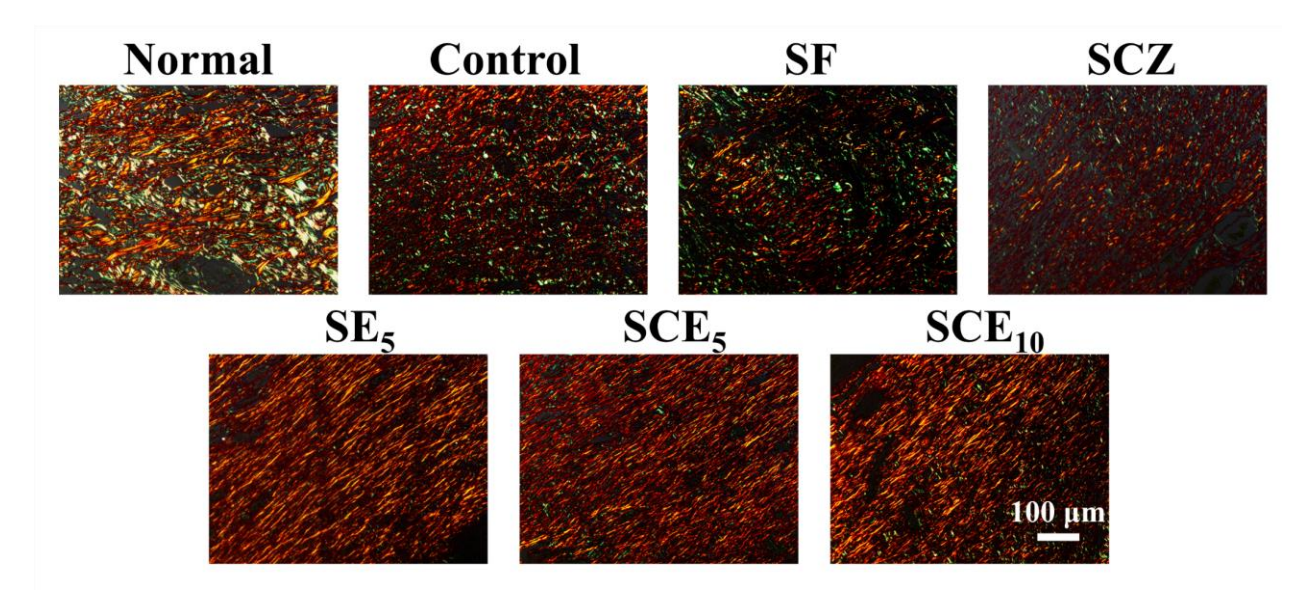


Fig. S9 Sirius red staining images of rat skin wounds of Normal, Control, SF, SCZ, SE₅, SCE₅, SCE₁₀ groups on day 14.

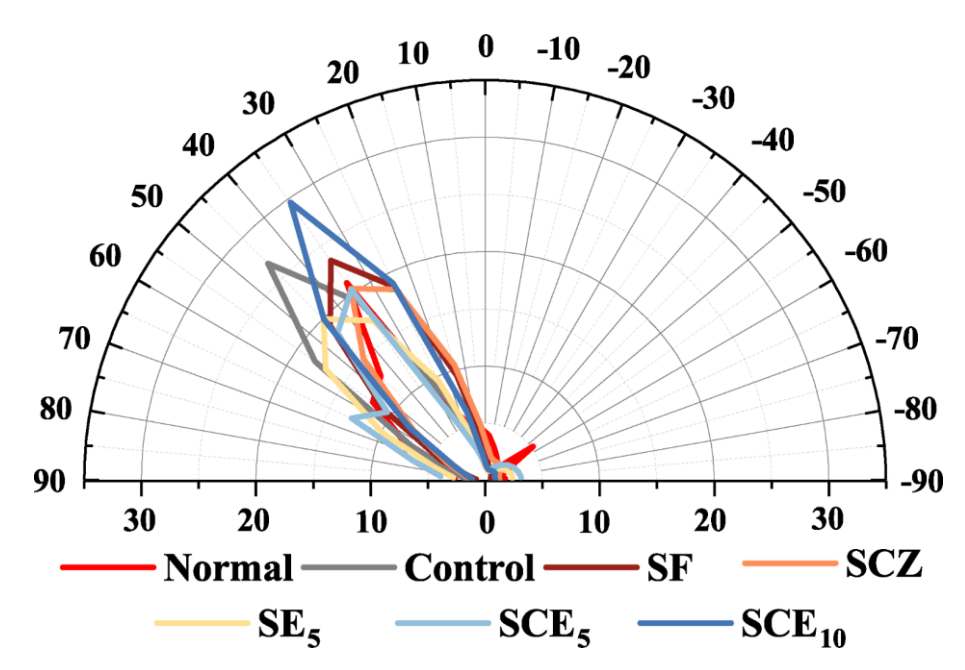


Fig. S10 Polar coordinates of collagen fiber orientation.



Fig. S11 a IL-1 β and **b** IL-10 immunohistochemical staining images of Control, SF, SCZ, SE₅, SCE₅, and SCE₁₀ groups on day 14.

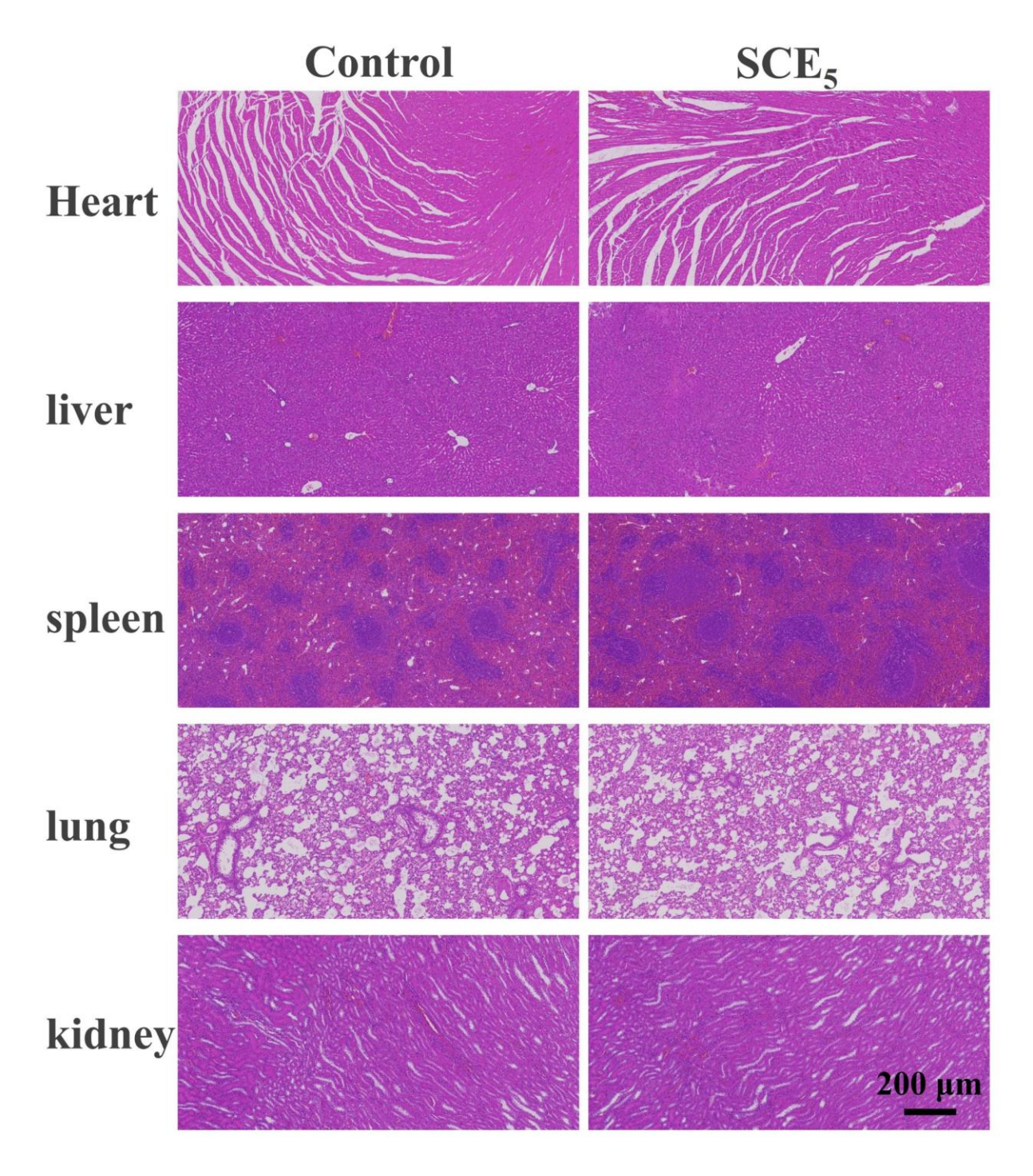


Fig. S12 Biological safety of Control and SCE₅ groups *in vivo* through H&E staining of heart, liver, spleen, lung, and kidney.

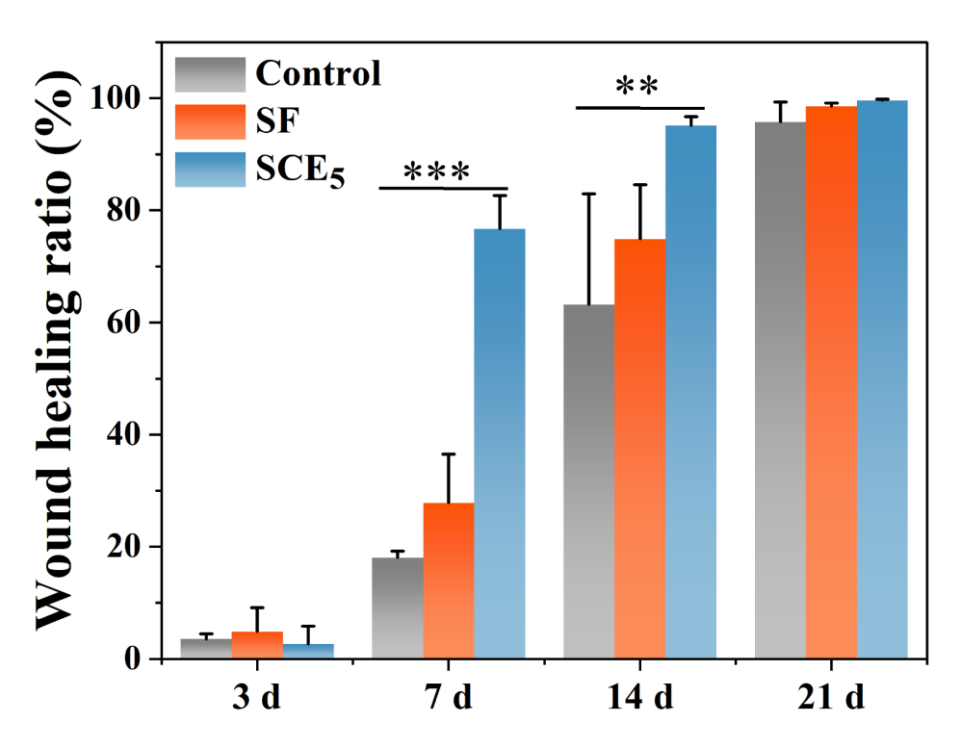


Fig. S13 quantitative statistical analysis of wound healing for rabbit ear wound (n =6). *p < 0.05, **p < 0.01, ***p < 0.001.

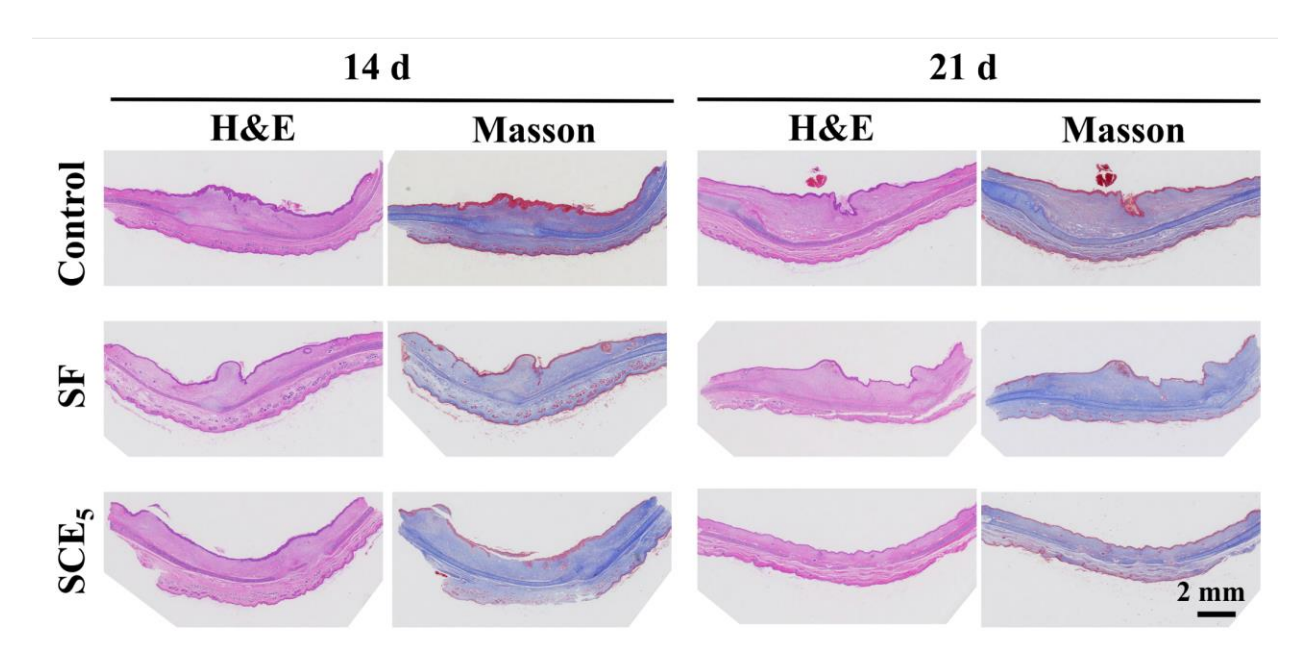


Fig. S14 H&E and Masson staining images of rabbit ear scar tissues of Control, SF, and SCEs groups on days 14 and 21.

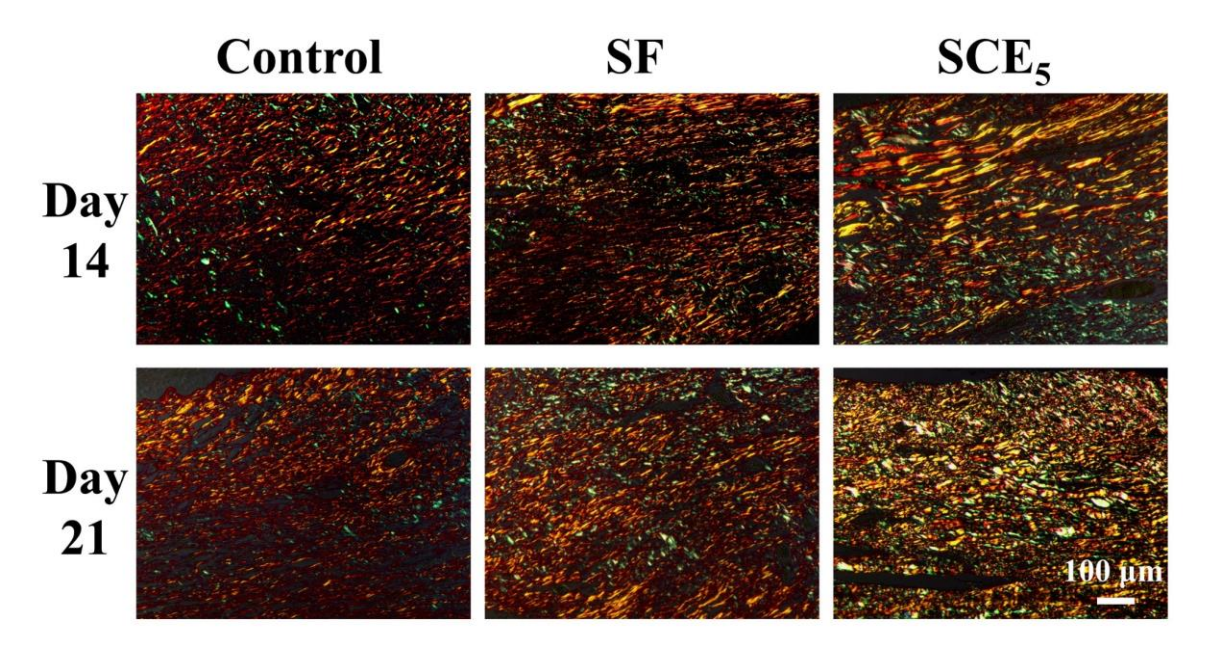


Fig. S15 Sirius red staining images of rabbit ear tissues of Control, SF, and SCE₅ groups on days 14 and 21.

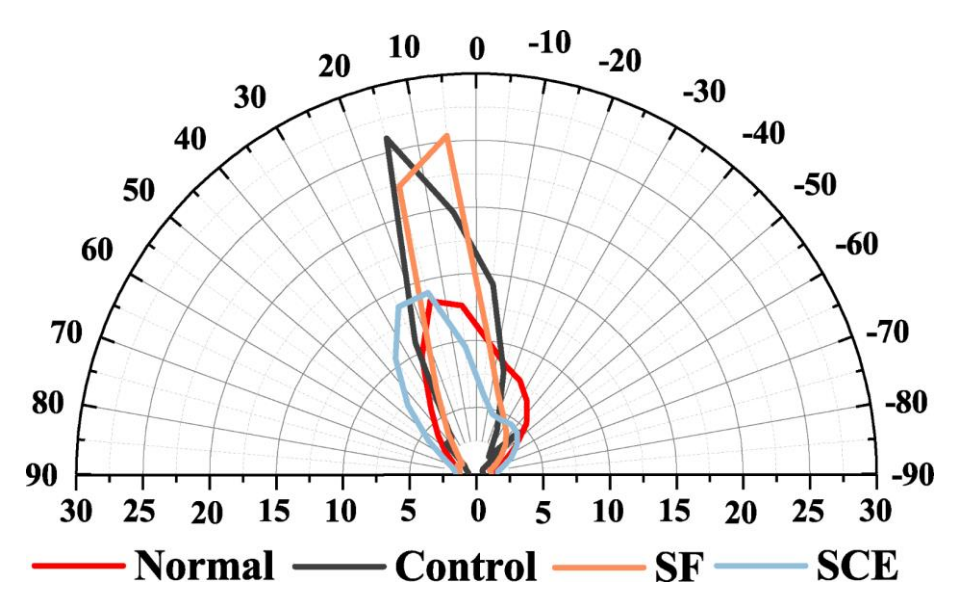


Fig. S16 Polar coordinates of collagen fiber orientation of rabbit ear tissues.

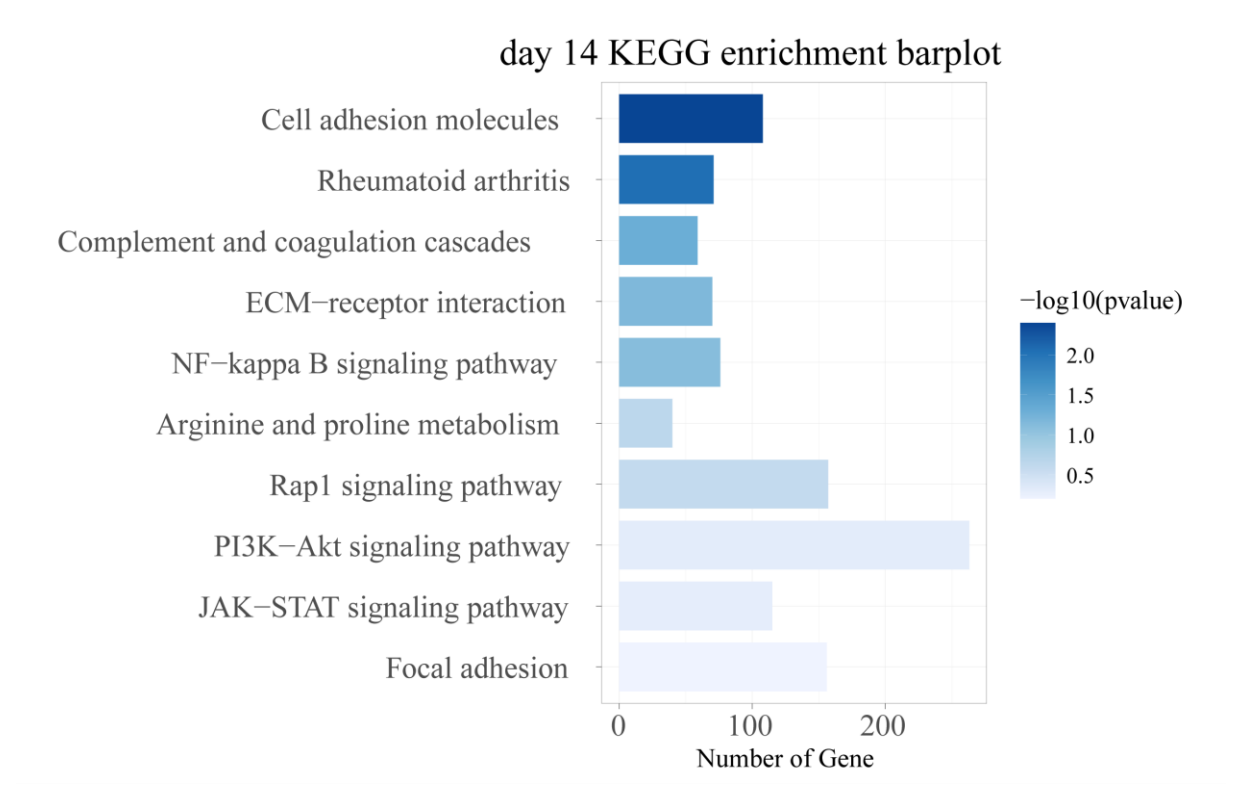


Fig. S17 Transcriptome KEGG pathway analysis results of rabbit ear skin tissues for Control and SCE groups on day 14.

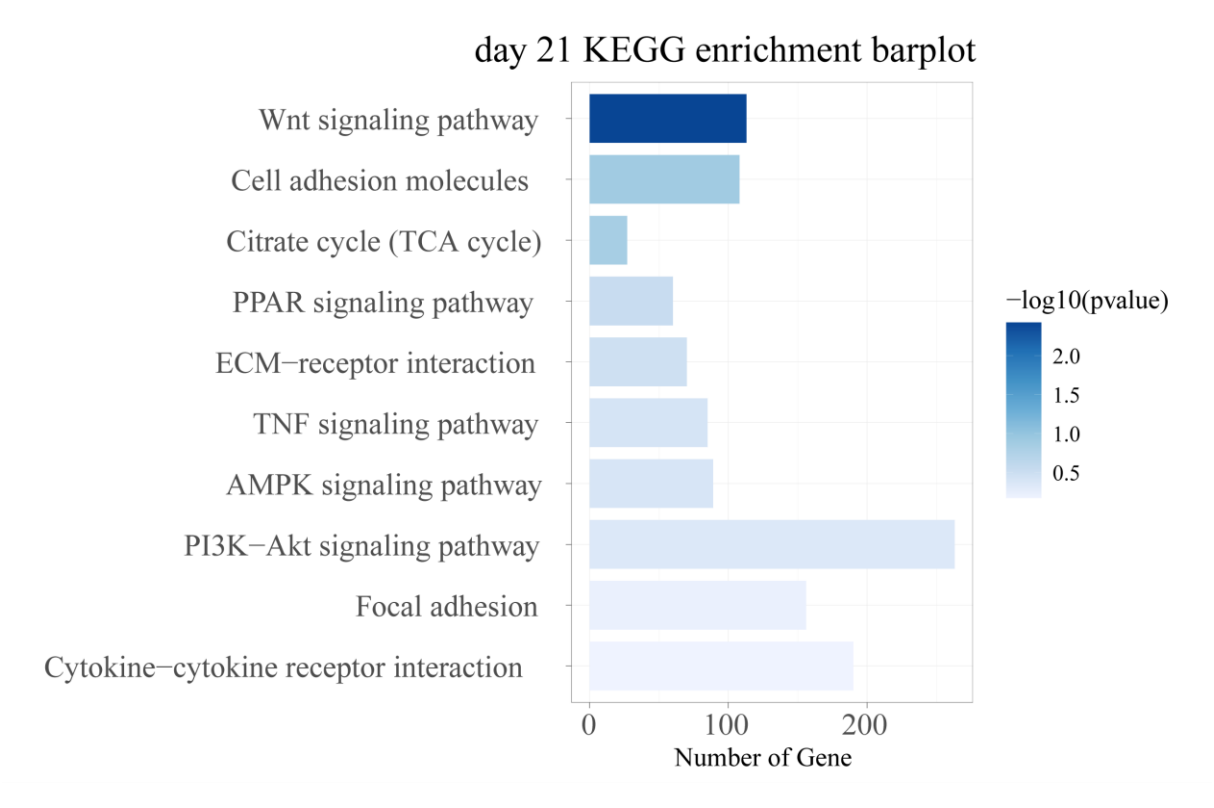


Fig. S18 Transcriptome KEGG pathway analysis results of rabbit ear skin tissues for Control and SCE groups on day 21.

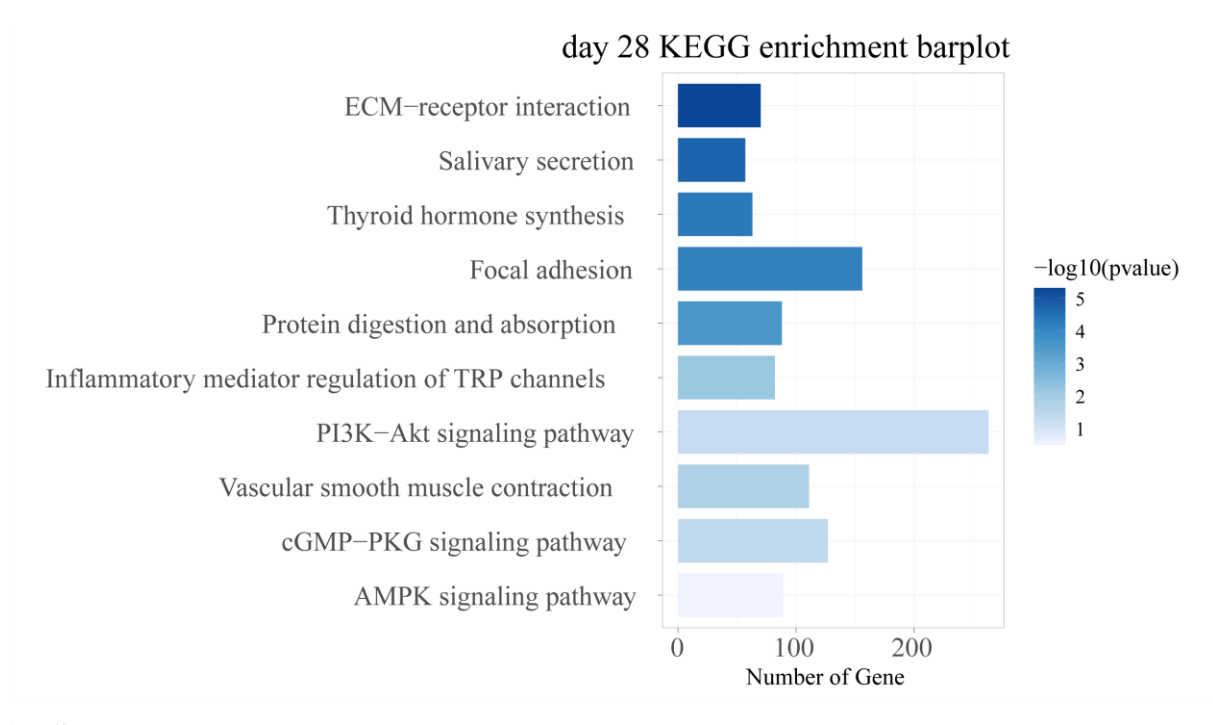


Fig. S19 Transcriptome KEGG pathway analysis results of rabbit ear skin tissues for Control and SCE groups on day 28.

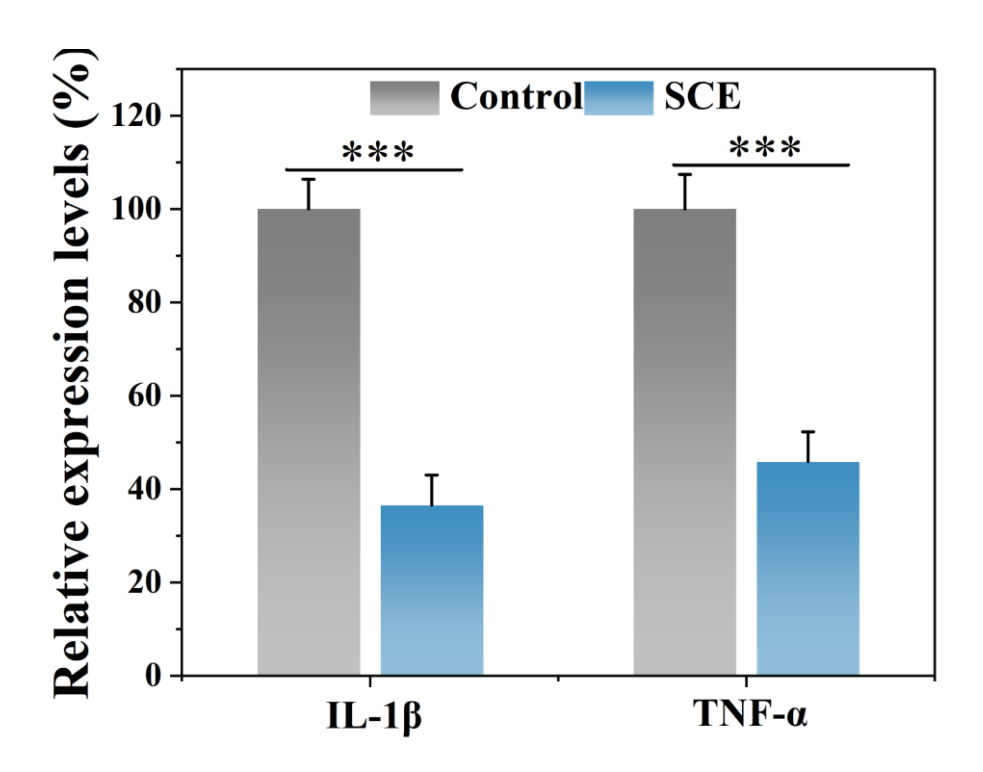


Fig. S20 Quantitative analysis results for IL-1 β and TNF- α of rabbit ear tissues (n = 3). *p < 0.05, **p < 0.01, ***p < 0.001.

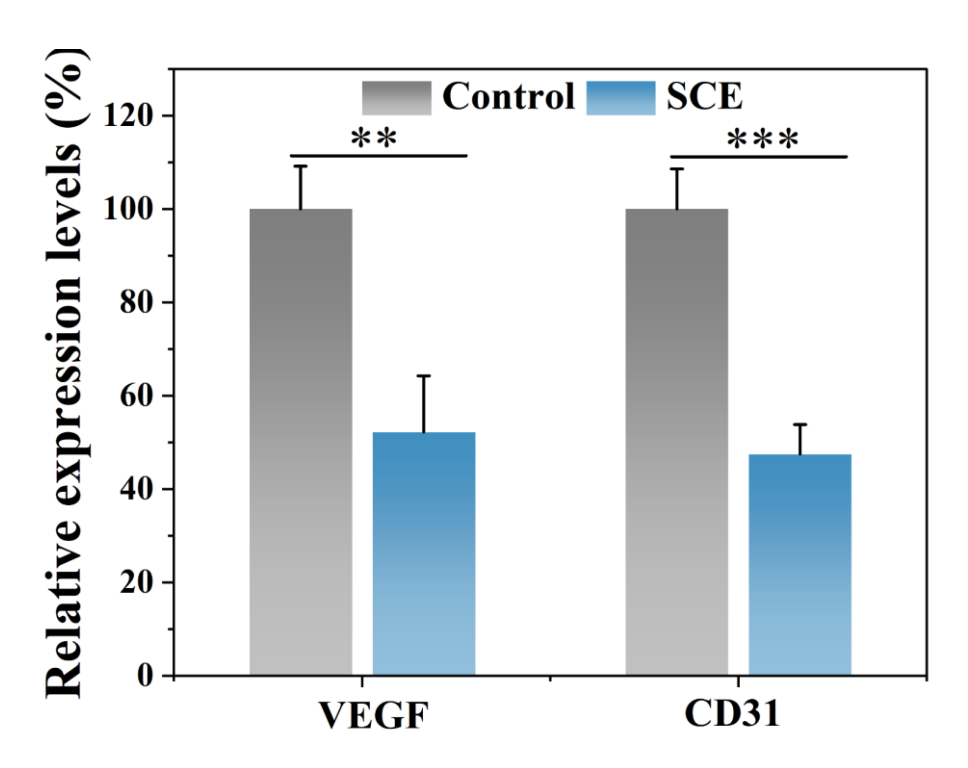


Fig. S21 Quantitative analysis results for VEGF and CD31 of rabbit ear tissues (n = 3). *p < 0.05, *p < 0.01, ***p < 0.001.

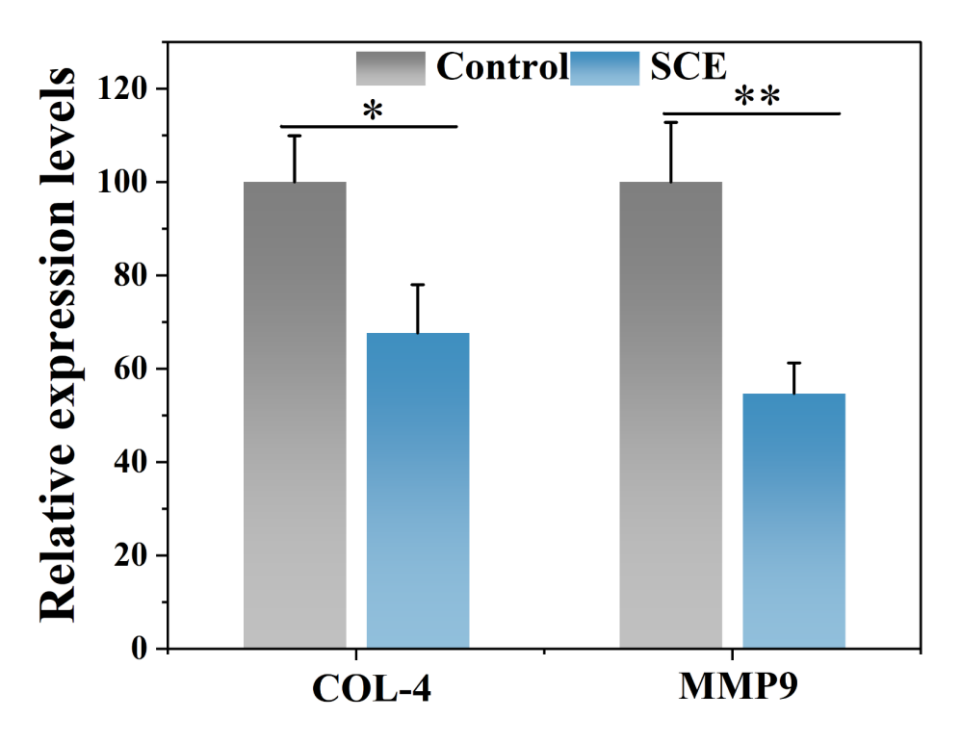


Fig. S22 Quantitative analysis results for COL-4 and MMP9 of rabbit ear tissues (n = 3). *p < 0.05, **p < 0.01, ***p < 0.001.

References:

- [1] Seo J-W, Kim H, Kim K, Choi SQ, Lee HJ. Calcium-Modified Silk as a Biocompatible and Strong Adhesive for Epidermal Electronics. . *Adv Funct Mater.* **2018**; 28: 1800802.
- [2] Wu M, Zhao Y, Tao M, Fu M, Wang Y, Liu Q, Lu Z, Guo J. Malate-Based Biodegradable Scaffolds Activate Cellular Energetic Metabolism for Accelerated Wound Healing. *ACS Appl Mater Interfaces*. **2023**; *15*: 50836.
- [3] Ju Y, Ma S, Fu M, Wu M, Li Y, Wang Y, Tao M, Lu Z, Guo J. Polyphenol-modified biomimetic bioadhesives for the therapy of annulus fibrosus defect and nucleus pulposus degeneration after discectomy. *Acta Biomater.* **2024**; *189*: 116.
- [4] Wang Y, Zhao Y, Ma S, Fu M, Wu M, Li J, Wu K, Zhuang X, Lu Z, Guo J. Injective Programmable Proanthocyanidin-Coordinated Zinc-Based Composite Hydrogel for Infected Bone Repair. *Adv Healthc Mater.* **2024**; *13*: e2302690.